Fluid circulation in the geothermal field of Tianjin (north-eastern China)

Angelo Minissale[1], Daniele Borrini[2], Giordano Montegrossi[1], Andrea Orlando[1], Franco Tassi[2], Orlando Vaselli[1,2], Antonio Delgado Huertas[3], Cheng Wanqing[4], Yang Jincheng[4], Cheng Xuzhou[5]

[1)] CNR (National Research Council of Italy) - Institute of Geosciences and Earth Resources, Via G. La Pira, 4 - 50121 Florence (Italy)

[2)] Department of Earth Sciences - University of Florence, Via G. La Pira, 4 - 50121 Florence (Italy)

[3)] Estación Experimental del Zaidín (CSIC), Prof. Albareda 1 - 18008 Granada (Spain)

[4)] Aode Renewable Energy Research Institute, 90 Weijin South Rd., Nankai District - 300381 Tianjin (China)

[5)] Institute of Nuclear and New Energy Technology, Tsinghua University, China

Tianjin geological map below Tertiary.

Thermal gradient (°C/100m)

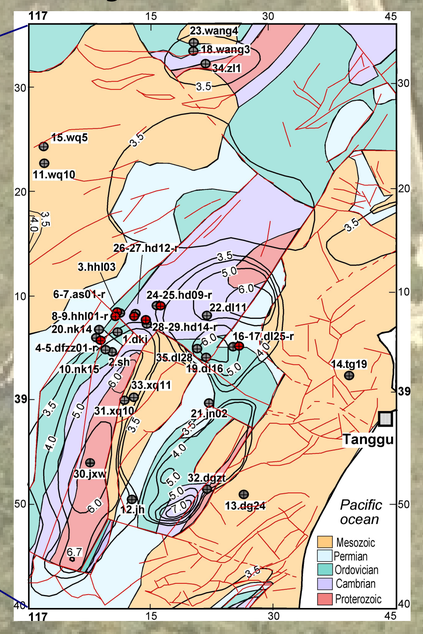

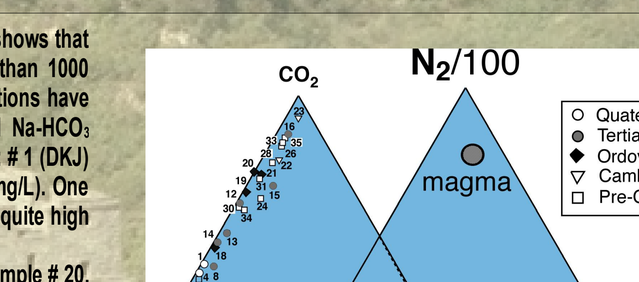

The Tianjin geothermal field is a typical low-enthalpy liquid-dominated convective system hosted in sedimentary formations, where maximum gradients are located in the "Cangxian" structural high of the pre-Tertiary formations around the city of Tianjin.

According to the temperature profiles at depth shown, it is evident that there are only few wells where the thermal gradient is higher (up to 6 °C/100 m: # 16 and 30) than the average Earth crustal gradient (about 3.3 °C m^{-2}), and that most wells have actually even lower thermal gradients (the lowest in well # 21: 2 °C m^{-2}). In particular, based on the temperatures measured in wells bottoming in the Tertiary and the Quaternary formations (# 1, 4, 8, 10, 12, 13, 14 and 15) the average shallow thermal gradient in the coastal area investigated in eastern China seems to be less than 3 °C m^{-2}. According to this finding, the Tianjing geothermal field must be considered as an excellent example of exploitation of a natural energy resource in a crust characterized by "*ordinary*" thermal flow.

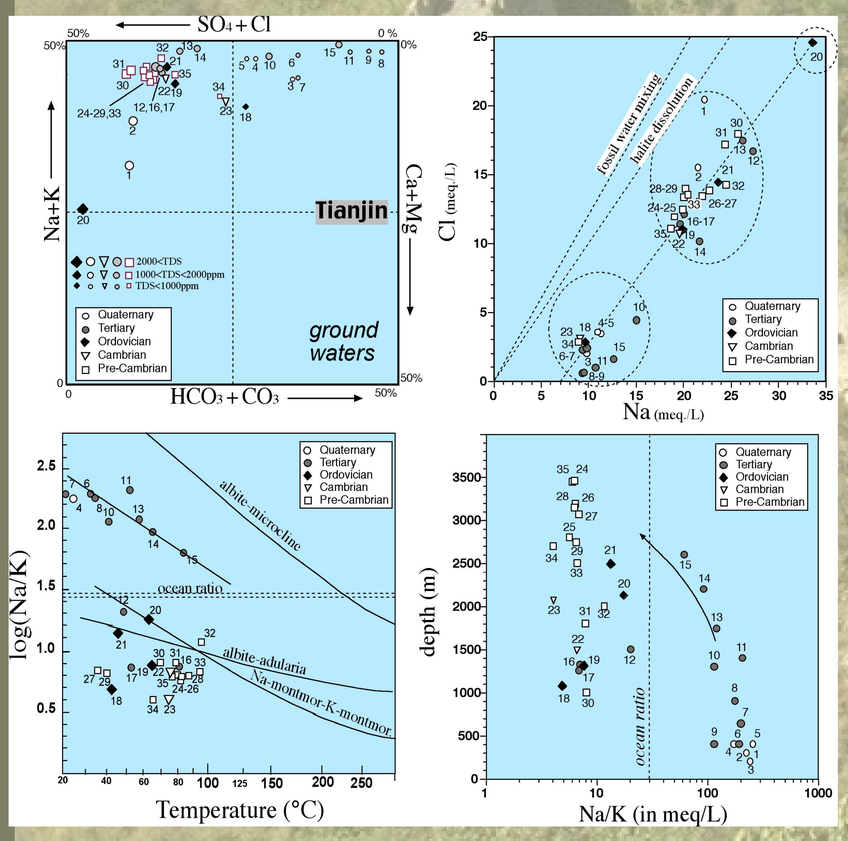

The diagram on the top left is the classic Langelier-Ludwig (1942) classifying diagram for waters. It shows that most samples from the Tertiary and the Quaternary sedimentary formations have salinity lower than 1000 mg/kg and have a prevalent Na-HCO_3 composition. Samples from the underlying pre-Tertiary formations have higher salinity (even more than 2000 mg/L) and a Na-Cl prevalent composition, with a marked Na-HCO_3 component. With respect to the remaining similar samples two shallow water samples (<200 m deep: # 1 (DKJ) and 2 (SH)) in the Quaternary sediments have Na-Cl composition, with higher salinity (up to 2000 mg/L). One sample from the Ordovician unit (# 20; NK14) has an anomalous prevalent Ca-SO_4 composition with quite high salinity (4700 mg/L).

The Na-Cl diagram on the top right shows that all samples, including the anomalous Ca-SO_4 sample # 20, are aligned along a line having similar Cl/Na ratio, but very different from those representing the ratio of seawater mixing (R=1.2) and the dissolution of halite (R=1), respectively. They are clearly clustered into two main groups, with different salinity: one including samples from the Tertiary and the Quaternary formations, the second including all samples from the underlying producing pre-Tertiary horizons. The distribution of the sample along a line having similar Na/Cl ratio suggests possible dilution and/or mixing between the two groups (or end-members).

In terms of water-rock interaction the *log*(Na/K)-temperature diagram at the bottom left (after Fournier 1991) indicates that these two important elements do not simply derive from any reasonable primary (albite and K-feldspar) or alteration (Na and K-montmorillonites) mineral assemblages, and also that their concentration is not simply due to mixing with ocean-type waters. This diagram is anyway able to show how different the waters hosted in the Tertiary and the Quaternary formations are, with respect to those hosted in the underlying formations, and that a couple of samples (# 23 and 34) do not belong to the Tertiary-Quaternary aquifer(s) even if they are located in the same formations, as already suggested by the Na-Cl diagram.

Finally, the Na/K vs. depth diagram gives the final interpretation of the main alkaline components in liquid phase, as follows. The two aquifers envisaged in the previous figures, having very different Na/K ratios, are present in the Tertiary-Quaternary formations and in the underlying pre-Tertiary formations, respectively. The one hosted in the Tertiary-Quaternary is present in depth up to 2500 m, whereas the one producing from the underlying formations rises up to 1000 m in the Tianjin structural high. There seem to be only a reduced mixing tendency of waters hosted in the Tertiary aquifer into the deeper pre-Tertiary aquifer and, this tendency, is anyway suggested by the upside bended arrow (bottom right).

All Tianjin samples are very well aligned along the line connecting the position of ASW and a gas formed in the crust (high radiogenic helium-4), although a little bit shifted with respect to the theoretical line reported at the base of the grey triangle. This position of samples suggests that the dissolved gas in the Tianjin water samples strictly derives from the exsolution of air-saturated waters and that there are no other sources of N_2, but air. The N_2/Ar ratio indeed resembles that of ASW (about 38). Nevertheless, in all gas samples there is a certain quantity of CO_2 of deep origin that, in some wells, is even up to 100% (# 16, 23).

Calcite saturation index

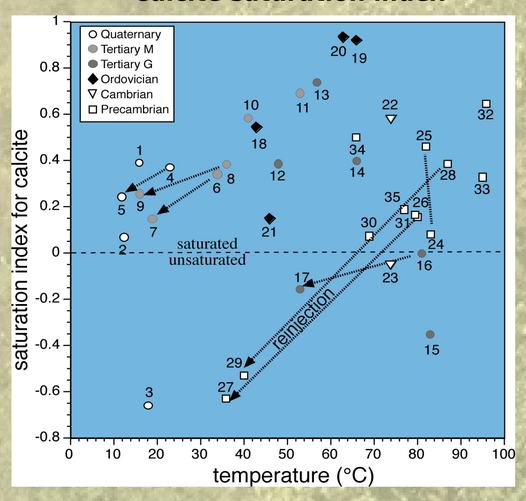

CO_2 degassing, the low pCO_2 and the ioncreased solubility of CO_2 at lower temperature make reinjected solutions unsaturated with respect to carbonates.

Conclusions:

- plugging by carbonates is very unlikely because of low pCO2 in solution
- plugging by quartz or silica is theoretically possbile where reinjection is carried out in low-Temperature wells
- plugging by iron and zinc hydroxides is possible and, although rather uncommon in geothermal systems, it is probably the main cause of reinjection problems
- physical plugging cannot be ruled out but it is largeley unquantified

Quartz saturation index

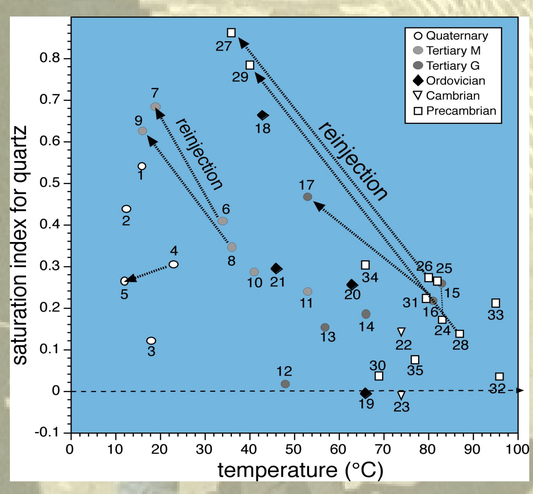

Quartz saturation is the real problem. Opposite to carbonates quartz saturation index strongly increases with decreasing temperature.

SATURATION-INDEX (log(Iap/K)) for minerals

	Sample	T °	Calc.	Arag.	Dolom.	F.Apat.	Apat.	Qrtz	Goeth.	Magnet.	Hemat.	Maghem.	Greenal.	Pyrit	ZnSiO3	Willemite
							$Ca_5(PO_4)_3F$		FeO(OH)	Fe_3O_4	Fe_2O_3	$Fe_{2.7}O_4$	$Fe_3Si_2O_5(OH)_4$			Zn_2SiO_4
1	DKJ	16	0,39	,238	0,935	2,14	16,37	0,542	2,81	7,69	7,59	-2,099	-3,087	10,77	3,91	2,006
2	SH	12	0,07	-0,08	0,286	0,43	13,87	0,434	4,38	12,08	10,71	1,265	0,887	14,04	2,92	0,204
3	HHL03	18	-0,6	-0,81	-1,175	-1,92	8,21	0,122	2,81	7,83	7,60	-2,243	-3,778	11,36	2,58	-0,275
4	DFZZ01	23	0,36	,222	0,781	1,58	14,20	0,305	5,68	16,14	13,37	3,131	3,635	12,02	4,86	3,976
5	DFZZ01-R	12	0,24	,087	0,297	1,08	14,87	0,264	4,82	13,64	11,59	2,228	2,711	nd	3,86	2,276
7	AS01-R	19	0,14	-0,01	0,493	<	<	0,684	<	<	<	<	<	<	3,45	0,863
8	HHL01	36	0,38	,245	0,328	1,53	12,44	0,345	5,80	16,54	13,66	2,466	2,564	12,09	4,28	2,486
9	HHL01-R	16	0,25	,102	-0,014	1,23	14,52	0,625	5,50	15,78	12,97	3,289	5,191	nd	4,29	2,686
10	NK15 zoo	41	0,58	,448	0,731	1,23	11,69	0,285	5,39	15,30	12,86	1,316	0,628	11,98	4,14	2,180
11	WQ10	53	0,68	,563	0,946	1,25	9,88	0,235	5,99	16,58	14,11	1,783	-0,614	12,47	4,14	1,991
12	JH	48	0,38	,255	0,620	<	<	0,016	6,23	17,64	14,56	2,554	1,265	12,64	4,34	2,695
13	DG24	57	0,73	,614	0,942	<	<	0,156	6,88	19,31	15,91	3,331	1,626	12,70	4,74	3,194
14	Tg19	66	0,39	,278	0,053	-0,30	5,81	0,186	6,13	17,36	14,44	1,317	-0,557	11,69	5,34	4,207
15	WQ5	83	-0,3	-0,46	-0,130	<	<	0,255	5,92	16,28	14,07	0,003	-3,986	9,54	6,40	5,967
16	DL25-BioP.	81	-0,1	-0,11	-0,401	<	<	0,215	5,13	14,33	12,50	-1,469	-5,046	10,06	4,73	2,701
17	DL25R	53	-0,1	-0,28	-0,393	<	<	0,465	5,72	16,10	13,57	1,242	0,044	<	7,06	7,588
18	WANG 3	43	0,54	,409	0,981	<	<	0,663	<	<	<	<	<	<	-0,80	-8,192
19	DL16	66	0,91	,800	1,556	<	<	-0,06	6,27	17,15	14,71	1,592	-2,392	11,79	5,01	3,734
20	NK14	63	0,93	,813	1,545	5,45	16,69	0,257	7,56	21,28	17,29	4,345	3,070	13,68	5,35	4,200
21	JN02	46	0,14	,016	0,220	<	<	0,295	5,73	16,13	13,56	1,683	0,493	17,38	-0,23	-6,679
22	DL11	74	0,57	,463	0,465	<	<	0,145	5,50	15,45	13,22	-0,363	-3,388	11,59	4,12	1,677
23	WANG-4	74	-0,1	-0,16	-0,447	<	<	-0,04	4,35	11,89	10,90	-2,678	-7,453	16,83	-2,56	-11,560
24	HD09	83	0,08	-0,03	0,074	<	<	0,175	5,71	16,04	13,66	-0,408	-3,641	10,51	4,98	3,216
25	HD09-R	82	0,45	,350	0,882	<	<	0,266	6,72	18,93	15,68	1,663	-0,766	<	6,32	5,825
26	HD12	80	0,15	,042	0,137	<	<	0,275	4,45	15,26	13,13	-0,784	-3,938	10,28	5,57	4,344
27	HD12-R	36	-0,6	-0,76	-0,975	<	<	0,864	4,51	12,54	11,08	-0,116	-0,661	<	4,27	1,954
28	HD14	87	0,38	,277	0,657	<	<	0,136	6,13	17,18	14,51	0,227	-3,174	9,57	6,51	6,251
29	HD14R	40	-0,5	-0,66	-0,950	<	<	0,784	4,24	11,82	10,57	-0,907	-1,838	<	3,94	1,291
30	JXW	69	0,07	-0,04	0,164	<	<	0,035	5,49	15,34	13,18	-0,117	-3,386	10,62	5,26	4,143
31	XQ10	79	0,15	,048	0,232	<	<	0,225	5,71	15,96	13,65	-0,262	-3,503	10,60	5,21	3,674
32	DGZT	96	0,64	,541	0,754	<	<	0,036	6,28	17,56	14,83	0,093	-3,893	11,73	4,49	2,178
33	XQ11	95	0,32	,222	0,313	<	<	0,216	6,05	16,91	14,37	-0,318	-4,039	10,16	5,73	4,490
34	ZL1	66	0,49	,380	0,834	<	<	0,306	6,10	17,17	14,39	1,263	-0,726	11,39	5,31	4,022
35	DL28	77	0,18	,073	0,308	<	<	0,076	6,00	16,94	14,21	0,461	-2,282	10,86	5,07	3,586

Saturation-Index for minerals and SEM analyses

	Sample	T °	calc.	qrtz	goeth.	magnet.	hemat.	pyrit.	$ZnSiO_3$	willemite	
					FeO(OH)	Fe_3O_4	Fe_2O_3	FeS_2	Zn_2SiO_4	*quantity*	*possible minerals*
1	DKJ	16	0,39	0,54	2,81	7,69	7,59	10,77	3,91	2,00	no solids
2	SH	12	0,07	0,43	4,38	12,08	10,71	14,04	2,92	0,20	?
3	HHL03	18	-0,6	0,12	2,81	7,83	7,60	11,36	2,58	-0,27	?
4	DFZZ01	23	0,36	0,30	5,68	16,14	13,37	12,02	4,86	3,97	no solids
5	DFZZ01-R	12	0,24	0,26	4,82	13,64	11,59	nd	3,86	2,27	no solids
7	AS01-R	19	0,14	0,68	<	<	<	<	3,45	0,86	HIGH
8	HHL01	36	0,38	0,34	5,80	16,54	13,66	12,09	4,28	2,48	no solids
9	HHL01-R	16	0,25	0,62	5,50	15,78	12,97	nd	4,29	2,68	?
10	NK15 zoo	41	0,58	0,28	5,39	15,30	12,86	11,98	4,14	2,18	no solids
11	WQ10	53	0,68	0,23	5,99	16,58	14,11	12,47	4,14	1,99	nd
12	JH	48	0,38	0,01	6,23	17,64	14,56	12,64	4,34	2,69	HIGH
13	DG24	57	0,73	0,15	6,88	19,31	15,91	12,70	4,74	3,19	MEDIUM
14	Tg19	66	0,39	0,18	6,13	17,36	14,44	11,69	5,34	4,20	MEDIUM
15	WQ5	83	-0,3	0,25	5,92	16,28	14,07	9,54	6,40	5,96	LOW
16	DL25-BioP.	81	-0,1	0,21	5,13	14,33	12,50	10,06	4,73	2,70	LOW
17	DL25R	53	-0,1	0,46	5,72	16,10	13,57	<	7,06	7,58	HIGH
18	WANG 3	43	0,54	0,66	<	<	<	<	-0,80	-8,19	no solids
19	DL16	66	0,91	-0,06	6,27	17,15	14,71	11,79	5,01	3,73	LOW
20	NK14	63	0,93	0,25	7,56	21,28	17,29	13,68	5,35	4,20	LOW
21	JN02	46	0,14	0,29	5,73	16,13	13,56	17,38	-0,23	-6,67	LOW
22	DL11	74	0,57	0,14	5,50	15,45	13,22	11,59	4,12	1,67	LOW
23	WANG-4	74	-0,1	-0,04	4,35	11,89	10,90	16,83	-2,56	-11,56	LOW
24	HD09	83	0,08	0,17	5,71	16,04	13,66	10,51	4,98	3,21	LOW
25	HD09-R	82	0,45	0,26	6,72	18,93	15,68	<	6,32	5,82	LOW
26	HD12	80	0,15	0,27	4,45	15,26	13,13	10,28	5,57	4,34	HIGH
27	HD12-R	36	-0,6	0,86	4,51	12,54	11,08	<	4,27	1,95	HIGH
28	HD14	87	0,38	0,13	6,13	17,18	14,51	9,57	6,51	6,25	LOW
29	HD14R	40	-0,5	0,78	4,24	11,82	10,57	<	3,94	1,29	HIGH
30	JXW	69	0,07	0,03	5,49	15,34	13,18	10,62	5,26	4,14	no solids
31	XQ10	79	0,15	0,22	5,71	15,96	13,65	10,60	5,21	3,67	LOW
32	DGZT	96	0,64	0,03	6,28	17,56	14,83	11,73	4,49	2,17	LOW
33	XQ11	95	0,32	0,21	6,05	16,91	14,37	10,16	5,73	4,49	MEDIUM
34	ZL1	66	0,49	0,30	6,10	17,17	14,39	11,39	5,31	4,02	LOW
35	DL28	77	0,18	0,07	6,00	16,94	14,21	10,86	5,07	3,58	HIGH